Table of Contents **S2**

Derivation of step-wise cooperativities of Cu binding to the CsoR tetramer

We begin by defining the ligand free, apo state, as M. If we assume that M binds ligand *x* with some equilibrium constant A_i, the following relationship is produced:

$$\mathrm{M} + \mathrm{x} \leftrightarrow \mathrm{Mx}\,;A_1 \quad (1)$$

where A_1 is the macroscopic binding constant for the binding of a single Cu(I) to any of four structurally identical sites. Equilibria analogous to that shown in eq 1 can then be written to reflect the formation of each differentially ligated species with 2, 3 or 4 *x* ligands bound, relative to the apo-state

$$\mathrm{M} + 2\mathrm{x} \leftrightarrow \mathrm{Mx}_2\,;A_2 \quad (2)$$
$$\mathrm{M} + 3\mathrm{x} \leftrightarrow \mathrm{Mx}_3\,;A_3 \quad (3)$$
$$\mathrm{M} + 4\mathrm{x} \leftrightarrow \mathrm{Mx}_4\,;A_4 \quad (4)$$

where A_2, A_3 and A_4 represent the macroscopic equilibrium constants for the binding of two, three and four ligands, respectively, to a non-dissociable apo-CsoR tetramer. We relate these equilibria to each other by means of the partition coefficient, *z*. This represents the sum of all species in solution with respect to the free ligand concentration, *x*:

$$z = 1 + A_1\mathrm{x} + A_2\mathrm{x}^2 + A_3\mathrm{x}^3 + A_4\mathrm{x}^4 \quad (5)$$

where we represent the unligated, or apo-state as the reference state (thus corresponding to the first term). A_i is related to the microscopic system by defining A_i in terms of microscopic variables. We define A_i as a function of the equilibrium association constant of each site *k*, cooperativity ω_i and statistical degeneracy, s_i, of the *i*th state. The average equilibrium association constant is known from previous work on this and related mesophilic CsoRs[1-3] with the step-wise cooperativities determined by the fitting the experimental data to the model. Statistical degeneracy for each *i*th state of ligation defined as follows for an *n*=4 ligand system is given as s_0=1, s_1=4, s_2=6, s_3=4, and s_4=1 for *i*=0-4 (Scheme S1)

$A_{0:1}$ → [0000]
$A_{1:1}$ → [1000] [0100] [0010] [0001]
$A_{2:1}$→ [1100] [1010] [1001] [0110] [0101] [0011]
$A_{3:1}$→ [1110] [1011] [1101] [0111]
$A_{4:1}$→ [1111]

Scheme S1

We first recast each A_i in terms of the statistical degeneracy, s_i, and assuming a single *k* and an ω that is independent of ligation state (Figure 1a, main text):

$$A_1 = 4k \quad (6)$$
$$A_2 = 6\omega k^2 \quad (7)$$
$$A_3 = 4\omega^2 k^3 \quad (8)$$
$$A_4 = \omega^3 k^4 \quad (9)$$

Substitution of eqs 6 through 9 into eq 5 then gives eq 10

$$z = 1 + 4kx + 6\omega k^2 x^2 + 4\omega^2 k^3 x^3 + \omega^3 k^4 x^4 \quad (10)$$

as representative of the simplest binding model. The concentration of each species is then given by 1/*z* (unligated M) and $A_i x_i/z$, where *i* ranges from 1-4, for each *i*th ligated state. Using these expressions, we simulated the experimental data and determined that this simple model overestimates the concentration of the *i*=3 state at all values of $\omega \geq 1$ since a single ω requires that the "peak" of the 1:1 and 3:1 complexes rise to the same relative degree, independent of the cooperativity parameter ω (data not shown) Thus, eqs 6-9 were expanded to include three ω_j values, denoted ω_1, ω_2 and ω_3 substituted for ω in eqs 7-9 respectively, to give

$$A_1 = 4k \quad (11)$$
$$A_2 = 6\omega_1 k^2 \quad (12)$$
$$A_3 = 4{\omega_2}^2 k^3 \quad (13)$$
$$A_4 = {\omega_3}^3 k^4 \quad (14)$$

Here, ω_1 is the average pairwise cooperativity for the *i*=2 state, ω_2 is the average pairwise cooperativity for the case where *i*=3, and ω_3 is the average pairwise cooperativity for the case of *i*=4. It is important to note that ω_i are step-wise parameters, and not microscopic cooperativities, since this method can *not* resolve the statistical degeneracies of each ligation state. We then derived expressions for the step-wise equilibrium constants, K_i , which defines each of four successive Cu-binding events,

$$K_1 = 4k \quad (15)$$
$$K_2 = \frac{3\omega_1 k}{2} \quad (16)$$
$$K_3 = \frac{2{\omega_2}^2 k}{3\omega_1} \quad (17)$$
$$K_4 = \frac{{\omega_3}^3 k}{4{\omega_2}^2} \quad (18)$$

We next used the nonlinear squares fitting function of Dynafit[4] to extract optimized values of K_i by allowing all four parameters to vary during the fit (continuous lines, Figure 3, main text). As expected, the absolute magnitude of K_i can *not* be uniquely defined by the data since these are essentially stoichiometric or "tight-binding" Cu(I) binding titrations, with resolved K_i dependent on the initial estimates for nonlinear least squares parameter optimization (see Figure S2; Table S1). However, the *relative* values of K_i and thus ω_i are robust and uniquely determined since these values are dictated only by the relative concentrations of all five states as a function of total Cu(I)

(Figure S2; Table S1). Eqs 15 through 18 were then solved for the cooperativities, ω_i, using these K_i values.

Materials and Methods

CsoR Sample Preparation*:* *B. subtilis* CsoR used in these experiments was expressed and purified as previously described.[1] Copper chloride (CuCl) was prepared as previously described[5] and titrated into apo-CsoR in an anaerobic glove box under argon gas at ambient temperature (23 ºC). Buffer exchange into 200 mM ammonium acetate was performed with Amicon® Ultra–0.5 3k microfilter devices (Millipore, Billerica, MA). Final protein concentrations were 125 μM tetramer, with the indicated total concentrations of Cu(I) added. Triplicate titrations were performed and subjected to the analysis outlined below.

Ion Mobility-Mass Spectrometry: Ion mobility spectrometry high resolution mass spectra were recorded using a Synapt G2S HDMS instrument at Indiana University (Waters Corporation, Manchester, United Kingdom). Instrument conditions were optimized for transmission and separation of large non-covalent complexes.[6] Briefly, samples were introduced into the source capillary at 30 µL/min with a kD Scientific syringe pump (KD Scientific Inc. Holliston, MA). Samples were ionized through ESI, with the source voltage set to 2.00 kV, with the sample cone at 30V and extraction cone at 50V. The trap gas was maintained at 2.0 mL/min, with the helium and nitrogen buffer gasses held at 180 mL/min and 90 mL/min, respectively. IMS wave velocity and height ranged at 150–250 m/s and 18–25V.

Surface Induced Dissociation Ion Mobility-Mass Spectrometry: SID experiments were carried out on a modified Synapt G2 HDMS instrument at the Ohio State University (Waters Corporation, Manchester, United Kingdom), outfitted with a homebuilt SID device with a fluorinated self-assembled monolayer on a glass surface coated with 10 Å of titanium and 1000 Å of gold (Evaporated Metal Films Corp., Ithaca, NY). The SID device was placed in front of the IMS cell to facilitate separation of the resulting fragments. (A similar set up, with the SID device after the IMS cell has been described.[7]) Solution and instrument conditions were similar to those in the IMS only measurements with the following changes: helium gas at 150 mL/min, nitrogen at 45 mL/min and IMS wave velocity at 350 m/s. nESI was carried out with a homebuilt source,[7] with voltages applied from 1.5kV to 1.8kV. Capillaries for nESI were made in house with a P-97 micropipette puller (Sutter Instruments, Navato, CA).

Data Analysis: All mass spectra were analyzed with Mass Lynx v4.1 (Waters Corporation, Manchester, United Kingdom) and OriginPro 9.0 (OriginLab Corporation, New Hampton, MA). Ion mobility spectra were analyzed with Drift Scope v2.4 (Waters Corporation, Manchester, United Kingdom). Modeling of experimental data was performed with Dynafit (BioKin, Ltd. Watertown, MA).[4]

Modeling mass to charge and CCS data with a set Gaussian functions: Cross section distributions for mobilities were modeled with a set of Gaussian functions using

the Peak Analyzer tool in OriginPro 9.0. Each gas phase conformation is represented by a Gaussian function, with the minimum number of gas phase conformations determined by the minimum number of Gaussian functions needed to fit the mobility distribution. FWHM and peak centers were varied iteratively until a set of values were found for modeling the data for the mobilities at each copper concentration. From here, the FWHM was fixed and the peak centers were only allowed to vary within the error for the calibrated cross sections. Peak amplitudes were varied until the model was fit. Residual sum of squares and coefficient of determination were both used to access the quality of the fit. This same protocol was applied to the mass spectra of the 14+, 15+, and 16+ CsoR tetramers to determine the relative abundance for the apo–, holo–, and partially Cu-ligated–tetramer states. Here the FWHM was fixed across all charge states so each species was constrained to the same width.

Calibration arrival time distributions into collision cross section distributions: Arrival time distributions acquired via travelling–wave IMS can be approximated into collision cross sections (CCS),[6,8-9] using proteins of known CCS values were measured on IMS instruments using a helium buffer gas and a uniform electric field as calibrants. Drift times (dt) for each charge state are obtained for the proteins and converted into corrected dt (dt') with eq 19:

$$dt' = \left(dt - \frac{C\sqrt{m/z}}{1000}\right) \quad (19)$$

C is an empirical factor for the Synapt,[6] and *m/z* is the mass-to-charge ratio for the specific ion. Known cross sections (Ω) obtained from literature are converted into corrected cross sections (Ω'), using eq 20:

$$\Omega' = \left(\frac{\Omega\sqrt{\mu}}{z}\right) \quad (20)$$

where μ is the reduced mass and z is the charge on the species of interest. The natural log of dt' and Ω' are plotted as a double linear regression to obtain a calibration curve. The slope (*X*) and y–intercept (A) are obtained from the equation of the best fit line. To obtain the calibrated cross section *X*, A and dt' of the ion of interest are used in eq 21:

$$\Omega = z\sqrt{\mu^{-1}}dt'^{X}e^{A} \quad (21)$$

The reported cross sections for individual charge states of ubiquitin and cytochrome *c* were obtained from the Clemmer Cross Section Database and used for cross section calibrations to give a regression R^2-value of 0.9924.[6,10-11] The calculated error for species of known cross section using the obtained calibration values was 0.7%.

Supplemental Tables

Table S1: Resolved K_1 values (nM^{-1}) (see Figure 1c, main text) for the species fractions vs. total Cu(I) (see Figure 3, main text) using various initial estimates for K_i parameter optimization using nonlinear least squares fitting with Dynafit.[4] The calculated values correspond to those continuous curves drawn through the raw data in Figure S1.

Equilibrium Constant	Initial Value (nM^{-1})	Calculated Value (nM^{-1})	Standard Error
K1	1.00E+09	1.76E+09	1.00E+08
K2	1.00E+09	1.27E+09	9.70E+07
K3	1.00E+09	8.05E+08	8.26E+07
K4	1.00E+09	3.00E+09	2.60E+08

Equilibrium Constant	Initial Value (nM^{-1})	Calculated Value (nM^{-1})	Standard Error
K1	1.00E+08	1.51E+08	8.59E+06
K2	1.00E+08	1.09E+08	8.30E+06
K3	1.00E+08	7.02E+07	7.16E+06
K4	1.00E+08	2.53E+08	2.17E+07

Equilibrium Constant	Initial Value (nM^{-1})	Calculated Value (nM^{-1})	Standard Error
K1	1.00E+10	1.40E+10	7.95E+08
K2	1.00E+10	1.00E+10	7.64E+08
K3	1.00E+10	6.41E+09	6.51E+08
K4	1.00E+10	2.33E+10	2.00E+09

Starting Equilibrium (nM^{-1})	ω_1	ω_2	ω_3
1.00E+09	1.9	2.3	5.2
1.00E+08	1.9	2.3	5.2
1.00E+10	1.9	2.3	5.2

Supplementary Figures:

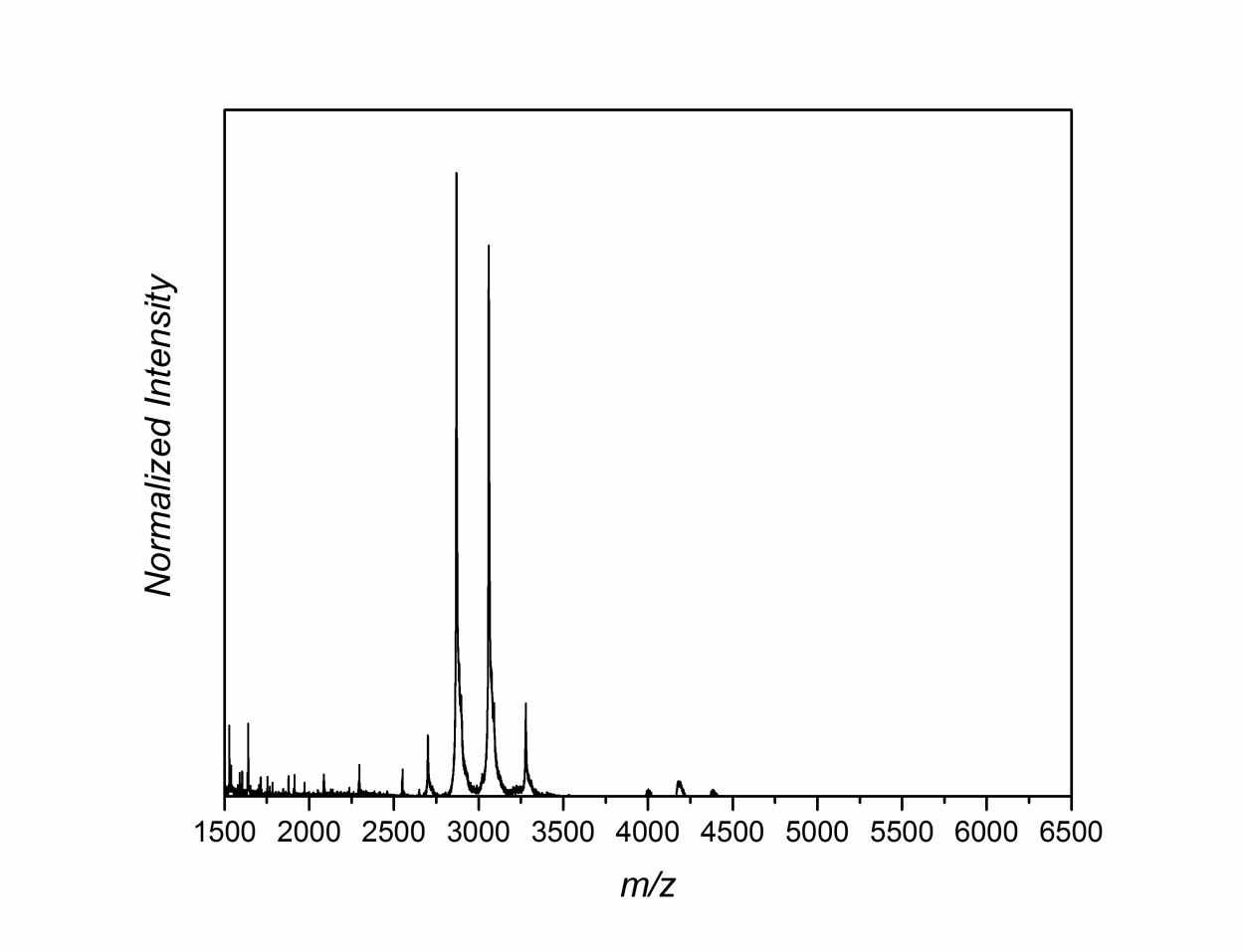

Figure S1: Mass to charge spectrum of apo CsoR. The spectrum is dominated by tetramer charge states, with small fractions (less than 5% of the total spectral intensity) of monomer, dimer and octamer present.

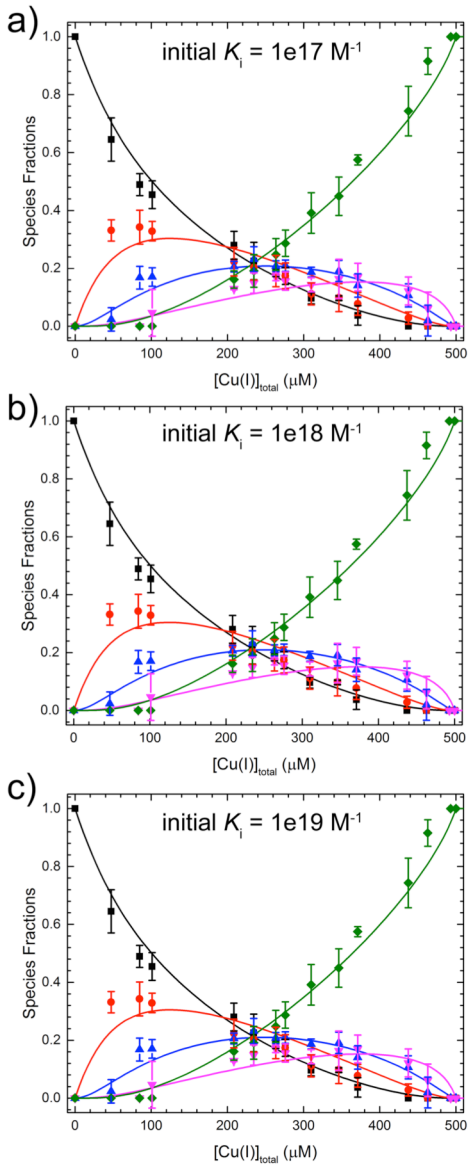

Figure S2: The nonlinear least squares global fit (continuous lines) to the species fractions vs. total Cu(I) curves can *not* be used to define K_i, with resolved K_i dependent on the initial (starting) value of K_i (shown). The continuous lines through each species fraction is defined by the calculated K_i given in Table S1. (a) initial K_i is 10^{17} M^{-1}, (b) K_i is 10^{18} M^{-1} and (c) K_i is 10^{19} M^{-1}. This is as expected since these are stoichiometric Cu(I) binding isotherms, with $[CsoR]_{total}>>1/K_i$. However, ω_i values are robustly determined since these values are dictated only by the relative species fractions of each of the five states as the tetramer is loaded with Cu(I) (Table S1).

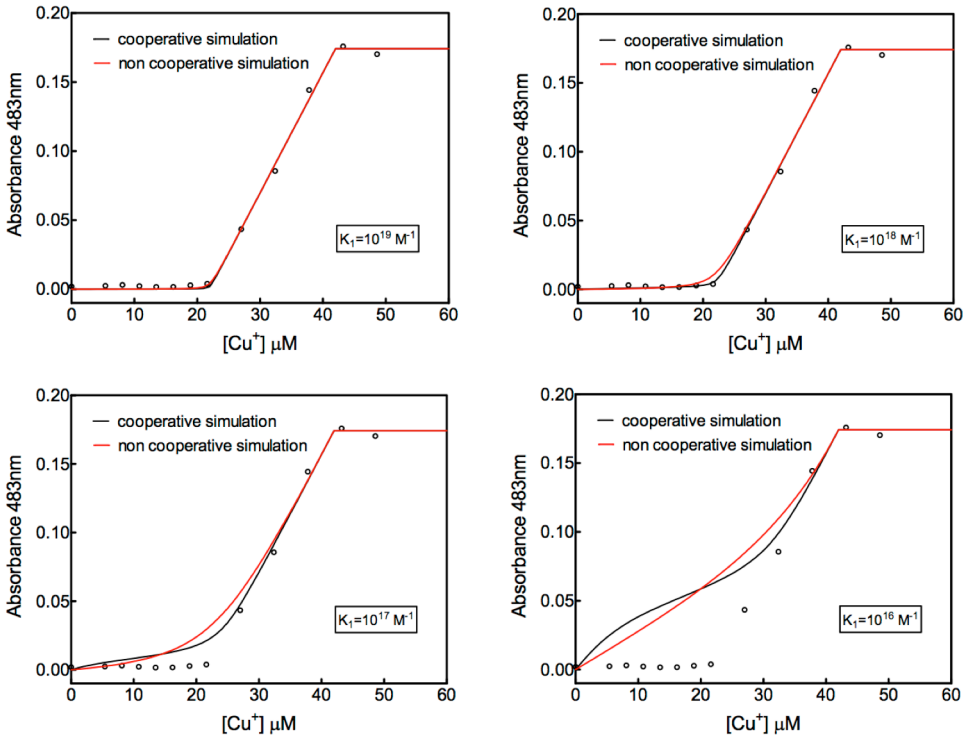

Figure S3: Simulated bathocuprione disulfonate (BCS) chelator competition binding curves defined by the non-cooperative (*red* continuous lines) and ligation-specific cooperative (*black* lines) binding models in which K (non-cooperative simulation) and K_1 (cooperative simulation) are set to be equal to the value given in each panel. Experimental data, A_{483} (corresponding to formation of the Cu(I):BCS$_2$ complex) vs. total Cu(I) added are shown as *open* circles for reference (22 µM apo *B. subtilis* CsoR protomer; 40 µM BCS).[1] The use of one binding model vs. the other can *not* be justified on the basis of these experimental binding curves alone since the binding is nearly stoichiometric ($K_{Cu} \geq 10^{19}$ M^{-1}); BCS is a relatively poor competitor. These two binding models can only be distinguished at lower K_i (see lower right).

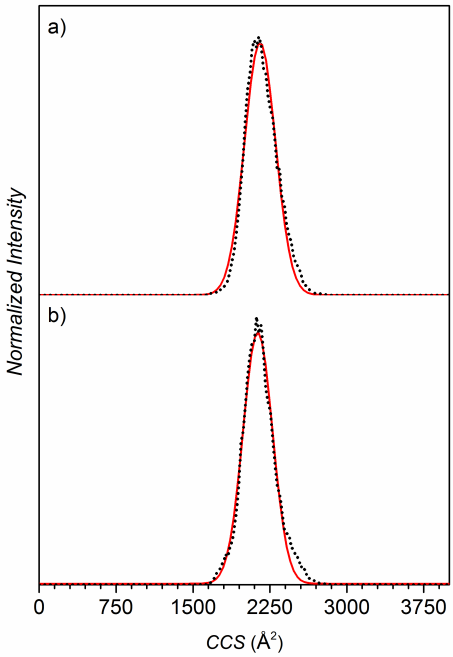

Figure S4: Collisional cross sectional distributions modeled with a single Gaussian curve for the apo (a) and holo (b) CsoR tetramers. The continuous line represented by the Gaussian model is *red*, while raw data are given by the *black* dotted line. Data are normalized to the peak intensity in each case. Peak centers are 2252 $Å^2$ for apo and 2231 $Å^2$ for holo CsoR tetramers, respectively. Spectral subtraction of the raw data (*black*) and fitted curve (*red*) is given in Fig. 5a, *top* panel, with the sum of the squares of the residuals shown in Fig. 5b, *top* panel.

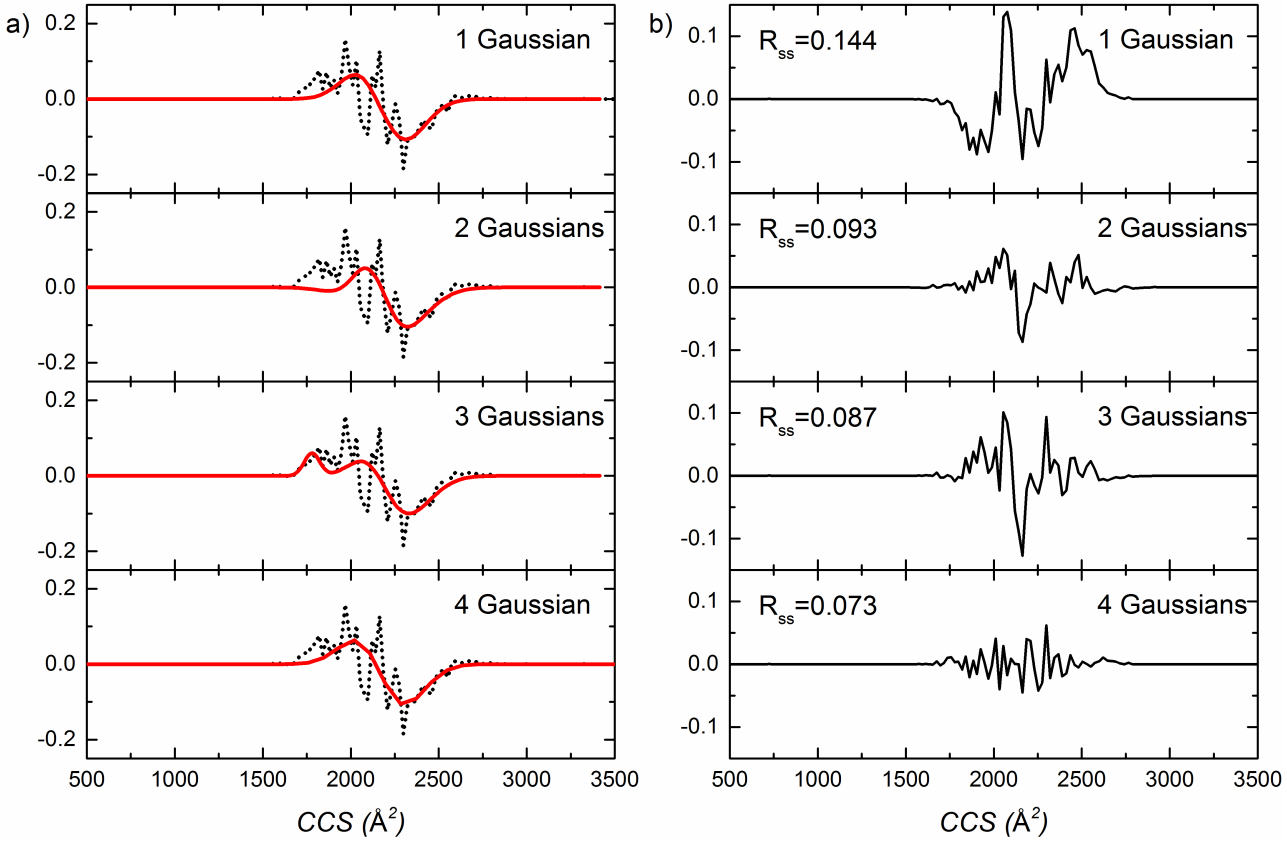

Figure S5: Subtraction of apo data from holo data for the raw mobility, superimposed with subtracted cumulative fit of Gaussians (a) residuals for Gaussian modeling with average residual sum of the squares (b). Raw data for subtraction is represented by continuous *black* dotted line and cumulative subtraction by the solid *red* line. Subtracted data show the cumulative fit is independent of the number of Gaussians, with holo CsoR fit always favoring a smaller CCS. The addition of a 5th Gaussian did not improve the residuals or the sum of squares of the residuals, suggesting that a fit of four (4) Gaussians is the best fit of these data.

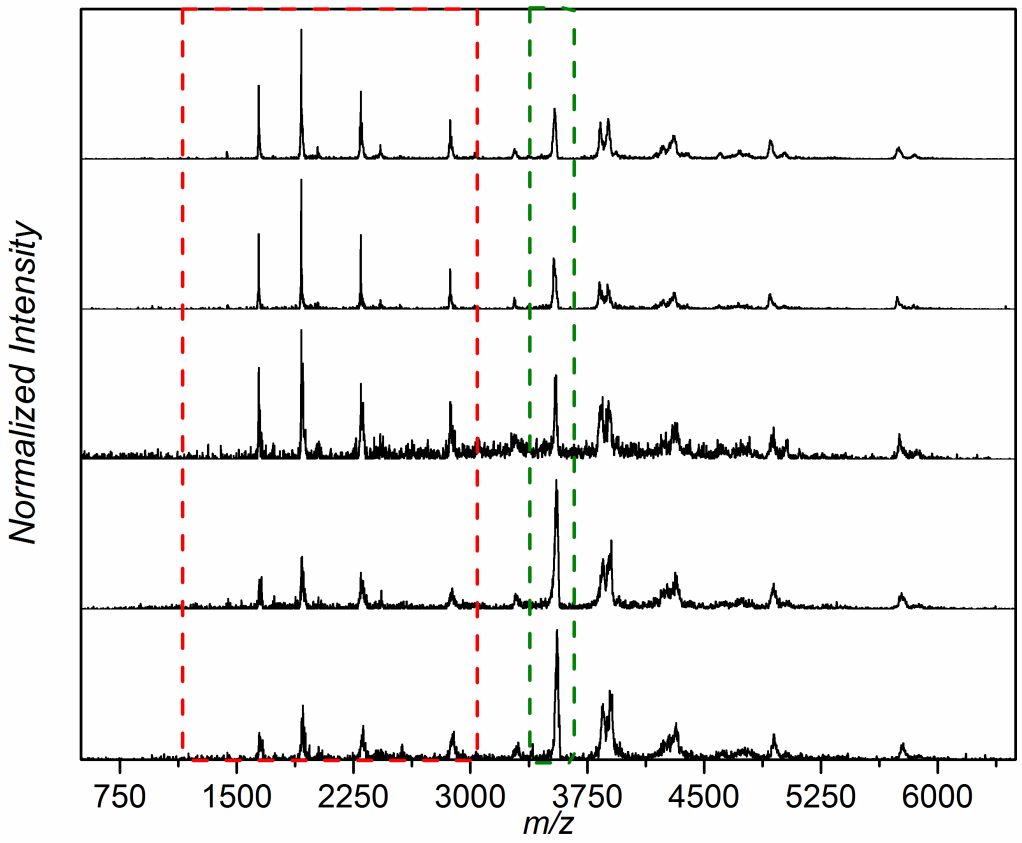

Figure S6: Resulting SID–IMS 13+ tetramer mass to charge spectra at an acceleration voltage of 40 V (520 eV) for apo CsoR (a), CsoR–1Cu(I) (b), CsoR–2Cu(I) (c), CsoR–3Cu(I) (d) and holo CsoR (e). Precursor ions were selected through mass selection with the quadrupole before the trap cell. Data are normalized to the intensity of the base peak. 125 μM CsoR tetramer solutions were titrated with stoichiometric concentrations of CuCl and buffered with 200 mM ammonium acetate. Precursor ions are highlighted in the *green* box, monomer fragments are highlighted in the *red* box.

Supplementary References

[1] Z. Ma, D. M. Cowart, R. A. Scott, D. P. Giedroc, *Biochemistry* **2009**, *48*, 3325-3334.

[2] Z. Ma, D. M. Cowart, B. P. Ward, R. J. Arnold, R. D. DiMarchi, L. Zhang, G. N. George, R. A. Scott, D. P. Giedroc, *J Am Chem Soc* **2009**, *131*, 18044-18045.

[3] N. Grossoehme, T. E. Kehl-Fie, Z. Ma, K. W. Adams, D. M. Cowart, R. A. Scott, E. P. Skaar, D. P. Giedroc, *J Biol Chem* **2011**, *286*, 13522-13531.

[4] P. Kuzmic, *Anal Biochem* **1996**, *237*, 260-273.

[5] Y. Fu, H. C. Tsui, K. E. Bruce, L. T. Sham, K. A. Higgins, J. P. Lisher, K. M. Kazmierczak, M. J. Maroney, C. E. Dann, 3rd, M. E. Winkler, D. P. Giedroc, *Nat Chem Biol* **2013**, *9*, 177-183.

[6] B. T. Ruotolo, J. L. Benesch, A. M. Sandercock, S.-J. Hyung, C. V. Robinson, *Nat Prot* **2008**, *3*, 1139-1152.

[7] M. Zhou, C. Huang, V. H. Wysocki, *Anal Chem* **2012**, *84*, 6016-6023.
[8] R. Salbo, M. F. Bush, H. Naver, I. Campuzano, C. V. Robinson, I. Pettersson, T. J. Jørgensen, K. F. Haselmann, *Rapid Commun Mass Spectrom* **2012**, *26*, 1181-1193.
[9] Y. Zhong, S.-J. Hyung, B. T. Ruotolo, *Analyst* **2011**, *136*, 3534-3541.
[10] K. B. Shelimov, D. E. Clemmer, R. R. Hudgins, M. F. Jarrold, *J Am Chem Soc* **1997**, *119*, 2240-2248.
[11] S. J. Valentine, A. E. Counterman, D. E. Clemmer, *J Am Mass Spectrom* **1997**, *8*, 954-961.